HA2-focused library

Medicinal and Computational Chemistry Dept., ChemDiv, Inc., 6605 Nancy Ridge Drive, San Diego, CA 92121 USA, Service: +1 877 ChemDiv, Tel: +1 858-794-4860, Fax: +1 858-794-4931, e-mail: ChemDiv@chemdiv.com

Influenza (flu) virus is the cause of major respiratory illness in humans resulting in 20,000–40,000 deaths annually in the United States alone [1] and killing millions in pandemic years. Viral subtypes are classified on the basis of the sequences of HA and neuraminidase (NA) surface proteins. Currently only strains of the H1N1, H3N2 subtypes and the B-type viruses circulate in human population. In recent years, however, certain strains of highly pathogenic avian influenza (H5N1) have been identified as the causative agents of a severe form of flu in humans, and it has been suggested that these have the potential to cause a pandemic [2].

Influenza viruses infect cells of the respiratory tract by first binding to the plasma membrane and then entering the cell through the endocytotic pathway. Hemagglutinin (HA) is an important and the most abundant influenza virus surface antigen (membrane glycoprotein) that is highly topical in influenza research and it is responsible for both binding and fusion. It contains two disulfide-linked polypeptide chains, HA1 and HA2-subunit, a relatively hydrophobic sequence of amino acids referred to as the fusion peptide. HA is the primary target of neutralizing antibodies during infection, and its sequence undergoes genetic drift and shift in response to immune pressure. Thus, it is constantly mutating, and consequently new vaccines must be developed each year against the new variants. Although HA2 is considerably more conserved than HA1 (Table 1, approximately 90% vs. 67% for Influenza A H1 and H3 subtypes in the surface-exposed regions) and might serve as a "universal" influenza vaccine candidate if it were to provide sufficient immunogenicity and protection), early mapping studies of antigenic regions on HA revealed that neutralizing antibodies are directed only against the receptor binding HA1 subunit [3]. HA2-interacting residues consisted largely of residues (7–46) and (290–321) of HA1 (Fig. 1).

Table 1. Fraction of exposed residues that are highly conserved in different HA fragments

	Influenza A						Influenza B		
	H1			H3					
	HA1, %*	HA2, %*	HA6, %*	HA1, %*	HA2, %*	HA6, %*	HA1, %*	HA2, %*	HA6, %*
Vaccine strains†	86	97	96	80	91	91	82	99	98
All strains‡	71	92	90	64	88	88	81	97	97

Residues that are at least 95% conserved and have accessibilities greater than 20% (exposed) were identified by mapping the percent conservation of the residues onto the structure of HA (PDB ID code 1HGD)

*Fraction of exposed residues that are ≥95% conserved. The total number of exposed residues in HA1, HA2, and HA6 is 146, 74, and 105, respectively.

†Sequences of the vaccine strains of the past 10 years were obtained from the NCBI Influenza Virus resource (6).

‡All the nonidentical, full-length HA sequences available at the NCBI flu resource were used for the analysis. The average conservation (in the exposed regions of HA) for H1 and H3 strains is 67%, 90%, and 89% for HA1, HA2, and HA6, respectively.

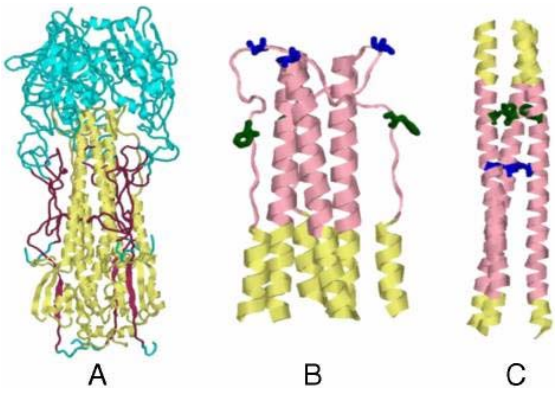

Fig. 1. Structures of the HA ectodomain. (A) Regions that are included in HA6 are shown in either maroon (HA1) or yellow (HA2). The rest of the molecule is shown in cyan. This figure was derived from the X-ray structure of HA from the (H3N2) isolate A/HK/68 (PDB ID code 1HGD) and was drawn using the program Rasmol. Conformation of residues (45–110) HA2 in the neutral pH (B) and low pH (C) structures of HA. The stretch 57–98 is shown in pink and the HA2 residues 63F and 73V, which are buried in the low pH form but are exposed in the neutral pH form, are shown in green and blue, respectively. Only a portion of the HA2 trimer (residues 45–110) is shown here for clarity.

Other studies have demonstrated that HA2-directed antibodies can provide protection in mice [4]. Recently, several neutralizing monoclonal antibodies have been isolated that bind the stem region of HA. These Abs have been shown to cross-react and neutralize several subtypes of viruses across clades and thus provide broad range protection [5]. These Abs act by targeting the HA2 region of the molecule and presumably prevent the conformational change of HA at low pH, thus blocking fusion of viral and host membranes. It is therefore speculated that an engineered antigen that could focus the immune response to these epitopes and elicit protection against viral infection could serve as the basis for a more universal vaccine.

At low pH within the endosome, HA undergoes large conformational changes that lead to fusion between the envelope and endosomal membrane, thereby allowing the viral nucleocapsid to pass into the cytosol [6]. The receptor binding HA1 subunit of HA shows much higher sequence variability relative to the metastable, fusion-active HA2 subunit, presumably because neutralizing antibodies are primarily targeted against the former in natural infection. Despite the never-ending mutations in HA, a stretch of 20, mostly nonpolar, amino acids is relatively well conserved. This segment must properly insert into the endosome membrane for fusion to occur and is known as the 'fusion peptide'. All viral fusion proteins contain fusion peptides, and they are a central motif in the mechanism of fusion. The fusion peptide is the only portion of HA that inserts into the target membrane and it does so only at low pH [7]. Point mutations in fusion peptides can block fusion [8]; the fusion peptide may have to insert into the endosome membrane with a precise structure for fusion to occur. In order to understand how this insertion

contributes to the perturbations of the lipid bilayer that are necessary for two membranes to fuse into one, the relevant structures must be known.

HA is a homotrimeric complex, with each monomer synthesized as a single polypeptide chain, HA0. After assembly into the trimeric form in the endoplasmic reticulum, each HA0 chain is posttranslationally cleaved by cellular proteases into two subunits, HA1 and HA2, which remain attached to each other by a disulfide bond [9]. HA1 is responsible for binding to host cell receptors, whereas HA2 is responsible for membrane fusion. In the uncleaved HA0, the fusion peptide is located in the interior of the amino acid sequence of the protein, but after cleavage it is precisely at the N-terminus of HA2. The portion of HA that resides outside the viral envelope contains the majority of the amino acid residues and is termed the ectodomain. Its structure — complete with fusion peptide — at neutral pH has been determined by X-ray crystallography [10]. The structure of a proteolytic fragment of the ectodomain at low pH has also been determined [11], but this fragment lacked the fusion peptide. Because the insertion of the fusion peptide into the endosome membrane at low pH is so central to the fusion process, the membrane-inserted structure is clearly needed to delineate the mechanism of fusion. However, addressing this problem has not been easy. At low pH, the fusion peptide of HA becomes exposed to the aqueous environment, significantly increasing the hydrophobicity of peptide fragments that contain it. Such peptides tend to aggregate at low pH and are difficult to crystallize [12], and thus X-ray crystallography is not a good option for studying the structure.

The fusion process

A general overview of fusion is shown in Fig. 2, in which only the HA2 portion of the hemagglutinin molecule is shown for clarity. This domain is critical both for setting the trigger for fusion and for destabilizing target membranes during the fusion process. A comparison of the neutral and low pH structures of HA shows that a loop (purple loop on top of HA2) at neutral pH becomes - helical at low pH [13], as had been anticipated [14]. This conversion presumably allows the fusion peptides to project toward the target membrane where they can then insert. Judging from the structure of HA at low pH [15], the fusion peptides should configure in a three-fold symmetric arrangement at the end of the central core of the trimer, and the transmembrane domains should pack around the core, in close proximity to the fusion peptides. Because the fusion peptides insert into the target membrane and the transmembrane domains are always spanning the viral envelope, the movements into the final three-fold symmetric configuration should bring the two membranes into close contact. The great majority of the experimental evidence favors the hypothesis that merging juxtaposed monolayers of two membranes (hemifusion) is an intermediate step that precedes formation of an HA-mediated fusion pore. For a pore to form, HA must somehow break the hemifusion connection that keeps the aqueous compartments separate. If the fusion peptides and transmembrane domains, inserted in different membranes, eventually come into direct

proximity and interact with each other as suggested by the crystal structure [16], they should disrupt the hemifusion connection [17] (Fig. 2).

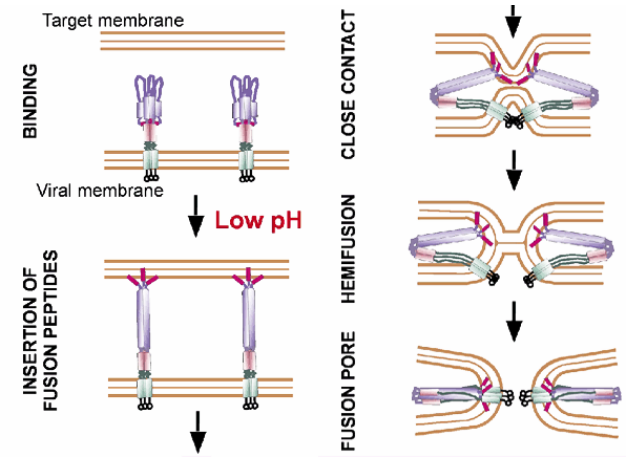

Fig. 2. The sequence of the HA conformational changes that are coupled to membrane fusion.

As shown in the figure, a virus binds to the plasma membrane via the HA1 subunit (not shown; only HA2 is shown for visual clarity). This subunit interacts with sialic acid on the cell surface. After the virus enters an endosome, low pH results in the extension of the triple-stranded coiled coil (*purple*) and the insertion of the fusion peptide (*red*) into the endosome membrane, leading to a conjectured extended conformation of HA2. HA2 reconfigures so that the coiled-coil is surrounded by the regions (*dark green* and *pink*; also forming three-fold symmetry) that continue toward the transmembrane domain (*light green*). This yields the structure that has been observed at low pH by X-ray crystallography. Because the fusion peptides and transmembrane domains are inserted in opposite membranes, the reconfiguration forces the membranes to come into close contact, hemifuse and then fuse. Variations of this scheme have been proposed by different investigators. Studies have shown that the cytoplamic tail of HA (*black*) is not important for fusion [18]. Because several HA trimers act in cooperation in the fusion process, it is probable that the rearrangements of lipids required for pore formation [19] are induced by the fusion peptides and transmembrane domains acting together as they accumulate at the hemifusion site. As a result, the virion enters the cell by endocytosis and is transported to the endosome, where the resulting acidic pH induces major conformational changes in the HA molecule, leading to exposure of the fusion peptide on the HA2 subunit and subsequent fusion of viral and endosomal membranes. The crystal structures of HA in the precursor, neutral pH, and low pH forms have been solved [20] and reveal the changes that occur upon cleavage and after the low pH conformational switch.

Therefore, fusion peptides appear to have multiple roles: grabbing onto the endosomal membrane so that it and the viral envelope can be pulled together, participating in the destabilization of contacting monolayers that leads to hemifusion, and perhaps facilitating pore formation itself. But HA trimers do not operate in isolation. Several HA trimers probably associate with each other to cause fusion. The initial

associations among intact HA trimers could possibly occur through hydrophobic interactions between their fusion peptides, since low pH causes the peptides to become exposed to the aqueous phase. The trimers may then coordinate so that each subsequent conformational change occurs in synchrony for all the trimers. Cooperativity of this type between HA trimers in a spatially localized region would theoretically facilitate fusion. Fusion peptides accumulate to high concentrations at the site of fusion, and they therefore may participate as an assembly, rather than as individual monomers, in the stages of fusion.

In the initial conformation of HA HA2 is locked in a metastable conformation by the receptor-binding HA1 subunit of HA. Acidification in the endosome triggers HA2 refolding toward the final lowest energy conformation. Recently, in [21], Kim and colleagues have explored structural properties as well as the fusogenic activity of the full sized trimeric HA2(1-185) that presents the final conformation of the HA2 ectodomain. Authors have found that HA2 mediates the fusion between lipid bilayers and between biological membranes in a low pH-dependent manner. Two mutations known to inhibit HA-mediated fusion strongly inhibited the fusogenic activity of HA2. At surface densities similar to those of HA in the influenza virus particle, HA2 formed small fusion pores but did not expand them. The obtained results confirm that the HA1 subunit responsible for receptor binding as well as the transmembrane and cytosolic domains of HA2 is not required for fusion pore opening and substantiate the hypothesis that the final form of HA2 is more important for fusion than the conformational change that generates this form.

Bommakanti et al [22] have designed an HA2-based immunogen using a protein minimization approach that incorporates designed mutations to destabilize the low pH conformation of HA2. The resulting construct (HA6) was expressed in *Escherichia coli* and refolded from inclusion bodies. Biophysical studies and mutational analysis of the protein indicate that it is folded into the desired neutral pH conformation competent to bind the broadly neutralizing HA2 directed monoclonal 12D1, not the low pH conformation observed in previous studies. HA6 was highly immunogenic in mice and the mice were protected against lethal challenge by the homologous A/HK/68 mouse-adapted virus. An HA6-like construct from another H3 strain (A/Phil/2/82) also protected mice against A/HK/68 challenge. Regions included in HA6 are highly conserved within a subtype and are fairly well conserved within a clade.

HA2 inhibitors

Currently available drugs for the prevention and treatment of seasonal influenza virus infections are the M2 ion channel blockers (amantadine and rimantadine) and the neuraminidase (NA) inhibitors (oseltamivir and zanamivir) [23]. The clinical usefulness of amantadine and rimantadine is limited due to the increasing incidence of adamantane-resistant viruses in the population [24]. Moreover, the M2 ion channel blockers inhibit only influenza A virus replication and are associated with neurological side effects. NA inhibitors are favored clinically, since they are effective against all NA subtypes, are well tolerated, and have a higher barrier for resistance [25]. However, drug-resistant isolates have been

detected in A/H3N2- and A/H5N1-infected patients receiving oseltamivir treatment [26]. Even more reason for concern is the recent and worldwide isolation of oseltamivir-resistant A/H1N1 mutants, even among untreated patients. Oseltamivir and, to a lesser extent, zanamivir have been stockpiled as part of pandemic preparedness plans and form the cornerstone of the response to the recent outbreak of the swine flu A/H1N1 virus [27]. However, it is unclear whether these antivirals will be sufficient to deal with larger influenza epidemics, so there is an urgent need to develop antivirals that act on a novel influenza virus target. Therefore, an alternative and very attractive antiviral strategy is to block influenza virus entry into the host cell, a process in which the viral HA plays a key role [28].

Numerous small molecules have been identified that block virus infectivity by inhibiting the conformational changes required for HA-mediated membrane fusion [29], and attempts have been made to "dock" some of them *in silico* to potential binding sites on HA. However, the development of more effective compounds has been limited by the lack of crystal structures of relevant HA complexes. Another potential limitation or disincentive to development for some of these compounds is that they appear to be effective against only certain subtypes of HA. Because the HAs of current seasonal influenza viruses, H1 and H3, are members of different phylogenetic groups, as are the highly pathogenic viruses of the H5 and H7 subtypes, it will be important to understand the structural basis of drug sensitivity and group specificity. Almost all HA2 inhibitors reported to date are peptide or peptide-based molecules. They disturb the crucial interaction between HA2-subunit and target-proteins in the host cell. However, several promising small-molecule HA2 inhibitors have also been developed and well described. For instance, Vanderlinden et al [30] have recently designed a novel class of *N*-(1-thia-4-azaspiro[4.5]decan-4-yl)carboxamide inhibitors (1-4) (Fig. 3) of influenza virus HA-mediated membrane fusion that has a narrow and defined SAR. Thus, in Madin-Darby canine kidney (MDCK) cells infected with different strains of human influenza virus A/H3N2, the lead compound, 4c, displayed a 50% effective concentration of 3 to 23 μM and an antiviral selectivity index of 10. No activity was observed for A/H1N1, A/H5N1, A/H7N2, and B viruses. The activity of 4c was reduced considerably when added 30 min or later postinfection, indicating that 4c inhibits an early step in virus replication. This compound and its congeners inhibited influenza A/H3N2 virus-induced erythrocyte hemolysis at low pH. The lead-compound-resistant virus mutants, selected in MDCK cells, contained either a single D112N change in the HA2 subunit of the viral HA or a combination of three substitutions, i.e., R220S (in HA1) and E57K (in HA2) and an A-T substitution at position 43 or 96 of HA2. The mutants showed efficiency for receptor binding and replication similar to that of wild-type virus yet displayed an increased pH of erythrocyte hemolysis. In polykaryon assays with cells expressing single-mutant HA proteins, the E57K, A96T, and D112N mutations resulted in the lead-compound resistance, and the HA proteins containing R220S, A96T, and D112N mutations displayed an increased fusion pH. Molecular modeling identified a binding cavity for 4c involving arginine-54 and glutamic acid-57 in the HA2 subunit. Our studies with the

new fusion inhibitor 4c confirm the importance of this HA region in the development of influenza virus fusion inhibitors.

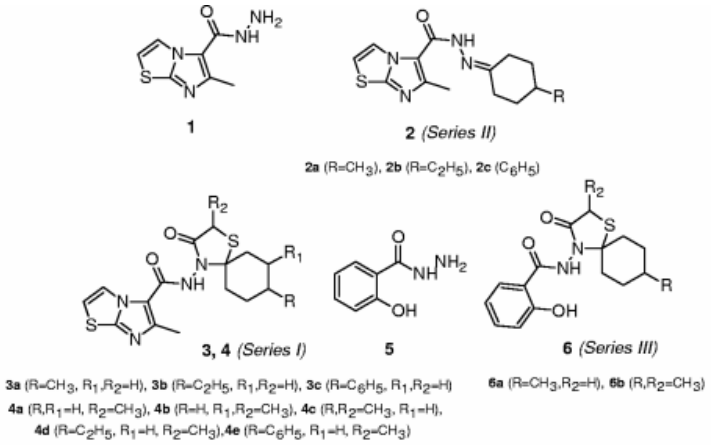

Fig. 3. *N*-(1-thia-4-azaspiro[4.5]decan-4-yl)carboxamide HA-inhibitors designed by Vanderlinden and colleagues

Analysis of the SAR revealed that the strongest antiviral activity was observed for the compounds 4c and 4d, in which the R substituent at position 8 of the spiro ring (Fig. 3) is a methyl and ethyl substituent, respectively. Both compounds had an average EC50 of 3.7 µM (Table 2).

Table 2. Activity in influenza A/H3N2 virus-infected MDCK cells

Compound[b]	R	R1	R2	Antiviral EC_{50}[c] (µM)				Cytotoxicity[d]		
				A/X-31		A/HK/7/87		MCC (µM)	CC_{50} (µM)	IC_{50} (µM)
				CPE	MTS	CPE	MTS			
Series I										
3a	Me	H	H	>100	>100	>100	>100	>100	ND	ND
3b	Et	H	H	>100	>100	>100	>100	>100	ND	ND
3c	Phe	H	H	>100	>100	>100	>100	≥100	ND	ND
4a	H	H	Me	100	100	>100	>100	>100	ND	ND
4b	H	Me	Me	32 ± 17	44	42 ± 4	40	>100	ND	ND
4c	Me	H	Me	3.3 ± 1.3	3.2 ± 2.0	5.0 ± 2.3	3.2 ± 2.3	≥100	>100	93
4d	Et	H	Me	2.4 ± 2.1	4.0 ± 3.8	4.2 ± 3.3	4.3 ± 3.0	50	>50	48
4e	Phe	H	Me	>100	>100	>100	>100	100	ND	ND
Series II										
2a	Me			>100	>100	>100	>100	≥100	ND	ND
2b	Et			>100	>100	>100	>100	>100	ND	ND
2c	Phe			>100	>100	>100	>100	>100	ND	ND
Series III										
6a	Me		H	>300	>300	>300	>300	≥60	>300	ND
6b	Me		Me	2.6 ± 2.3	5.9 ± 4.3	2.8 ± 1.8	1.4 ± 0.6	>50	>50	38
Oseltamivir carboxylate				0.0042 ± 0.0035	0.020 ± 0.040	1.7 ± 1.9	0.63 ± 0.23	>100	>100	80
Ribavirin				9.9 ± 3.3	11 ± 4	7.4 ± 2.1	7.2 ± 3.8	61 ± 30	>100	18

[a]The data shown are the means ± standard deviations of 2 to 7 independent tests. ND, not done. MDCK cells, Madin-Darby canine kidney cells; Et, ethyl; Me, methyl; Phe, phenyl; [b]Figure 3 shows the basic structures of the *N*-(1-thia-4-azaspiro[4.5]decan-4-yl)carboxamide compounds, series I, II, and III; [c]Antiviral activity is expressed as the EC_{50}, defined as the compound concentration producing 50% inhibition of virus replication, as estimated by microscopic scoring of the CPE or by measuring cell viability in the formazan-based MTS assay; [d]Cytotoxicity is expressed as the MCC, the compound concentration producing minimal changes in cell morphology, as estimated by microscopy; the CC_{50}, estimated by the MTS cell viability assay; or the IC_{50}, determined by cell counting.

Compound 4c showed minimal cytotoxicity at the highest concentration tested (100 μM), yielding a selectivity index (SI) (defined as the ratio of MCC to EC_{50}) of 27. 4d had a lower SI of 14. The importance of the substituent at position 8 was evident from the data showing that 4b, which has a methyl group at position 7 (R1) (Fig. 3) instead of 8, was 11-fold less active than 4c, while the compounds having no substituent (4a) or an 8-phenyl group (4e) were devoid of antiviral activity. Likewise, the methyl substituent in the spiro ring (R2) (Fig. 3) was shown to play an important role, since the analogues of 4c and 4d lacking this function (3a and 3b, respectively) were inactive. Similarly, removal of the spiro ring was found to be deleterious (compounds 2a, 2b, and 2c). A few compounds were synthesized with variations in the aromatic system. Substitution of the imidazo[2,1-b]thiazole ring (4c) by an o-hydroxyphenyl ring (6b) resulted in a minimal increase in antiviral activity; however, 6b was also more cytotoxic. The analogue lacking the methyl in the spiro ring (6a) was inactive. In contrast to the promising activities of 4c, 4d, and 6b against influenza A/H3N2 virus, these compounds were completely inactive against A/H1N1 and B viruses. The class of *N*-(1-thia-4-azaspiro[4.5]decan-4-yl)carboxamide inhibitors shows specific activity against influenza A/H3 viruses. This is surprising, since the backbone structure of our inhibitors is related to that of some HA1- and HA2-specific inhibitors, consisting of an aromatic system linked to a nonaromatic cyclic system via an amide bridge [31], therefore analogues of this series can be reasonably regarded as potential HA2-inhibitors.

For the different HA residues associated with 4c resistance, the calculated solvent accessibility was at least 100 $Å^2$ for A432 and E572, whereas R2201, A962, and D1122 had values of 20 $Å^2$ or less [32]. Docking experiments with 4c (after removal of TBHQ) were therefore restricted to A432 and E572, using Autodock 4 software and a grid size of 50 by 50 by 50 points and 0.375-Å resolution (Fig. 4).

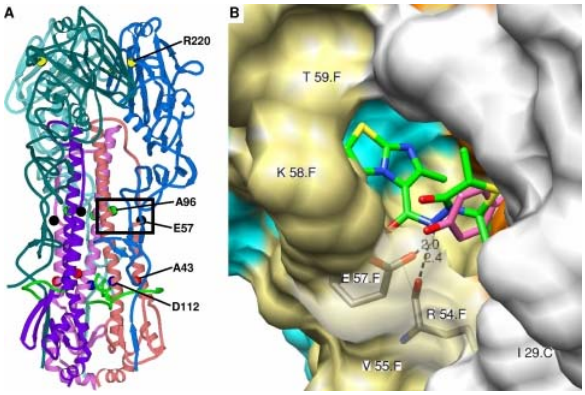

Fig. 4. Positions of 4c-associated HA mutations and the predicted binding pocket of 4c in the HA protein. The modeling was based on the published crystal structure of the X-31 HA in complex with TBHQ. (A) Ribbon diagram showing the locations of the amino acid residues (R2201, A432, E572, A962, and D1122) involved in 4c resistance. The HA1 chains are colored in sky blue (A chain), royal blue (C chain), and slate blue (E chain); HA2 chains are in pink (B chain), flesh (D chain), and purple (F chain); and the fusion peptide is indicated in green. The frame indicates the position of the binding pocket of 4c. (B) Chimera model of the interactions of 4c in the binding pocket around glutamic acid-57. The numbering of the amino acid residues includes the polypeptide chain (HA1 chains, A, not visible; C, white; and E, cyan; HA2 chains, B, not visible; D, orange; and F, khaki). Predicted hydrogen bonds with the main chain carbonyl of R542 and the side chain carboxyl of E572 are shown as dashed lines, with the distance indicated in angstroms. Residues I291, R542, V552, K582, and T592, indicated on the protein structure, and residues P2931, K3071, Y942, E972, L982, L992, and A1012 (not visible) are involved in hydrophobic interactions with 4c (shown in green; note that the cyclohexane part is not displayed). The predicted position of the N-(1-thia-4-azaspiro[4.5]decan-4-yl)carboxamide moiety of 4c is similar to that of TBHQ (shown in purple). 4c-specific hydrophobic interactions were observed between its imidazo[2,1-b]thiazole part and residues P2931, K3071, K582, and T592.

When all protein residues were kept rigid, no specific interactions between 4c and E57(F) (HA2 subunit) were observed. Superposition of chains B, D, and F showed that the orientation of the side chain of E57 differed among the three monomers, implying that this E57 residue is flexible and adopts different rotameric states. From these, we selected rotameric state ($\chi1$ = 49,84, $\chi2$ = 74.84, $\chi3$ = 160.79), which orients the glutamic acid side chain in the direction of the cavity, for 4c docking. After docking, the top 50 of docked ligand conformations were examined, and the highest-score conformation was selected based on the following criteria: specific hydrogen bonding with the E57(F) side chain and hydrophobic interactions with the R and R2 methyl groups of 4c. Interactions (H bonds and hydrophobic) were calculated using Ligplot and HBPlus, and the three-dimensional (3D) models were generated with UCSF Chimera.

Recently, Liu et al [33] have designed a novel small-molecule compound - CL-385319, an N-substituted piperidine. It is effective in inhibiting infection of H1-, H2-, and to a lesser extent, H3-typed influenza A viruses by interfering with the fusogenic function of the viral hemagglutinin. It has been shown that CL-385319 is effective in inhibiting infection of highly pathogenic H5N1 influenza A virus in Madin-Darby Canine Kidney (MDCK) cells with an IC(50) of 27.03±2.54 μM. This compound with low cytotoxicity (CC(50)=1.48±0.01 μM) could also inhibit entry of pseudoviruses carrying hemagglutinins from H5N1 strains that were isolated from different places at different times, while it had no inhibitory activity on the entry of VSV-G pseudotyped particles. CL385319 could not inhibit N1-typed neuraminidase activity and the adsorption of H5-typed HA to chicken erythrocytes at the concentration as high as 1 mg/ml (2.8 μM). Computer-aid molecular docking analysis suggested that CL-385319 might bind to the cavity of HA2 stem region which was known to undergo significant rearrangement during membrane fusion. Pseudoviruses with M24A mutation in HA1 or F110S mutation in HA2 were resistant to CL-385319, indicating that these two residues in the cavity region may be critical for CL-385319

bindings. These findings suggest that CL-385319 can serve as a lead for development of novel virus entry inhibitors for preventing and treating H5N1 influenza A virus infection.

A known inhibitor of membrane fusion and virus infectivity - tert-butyl hydroquinone (TBHQ) is another example of HA2 small-molecule inhibitors [[34]]. The structure of HA in complex with TBHQ clearly shows that the inhibitor binds in a hydrophobic pocket formed at an interface between HA monomers. Occupation of this site by TBHQ stabilizes the neutral pH structure through intersubunit and intrasubunit interactions that presumably inhibit the conformational rearrangements required for membrane fusion. The nature of the binding site suggests routes for the chemical modification of TBHQ that could lead to the development of more potent inhibitors of membrane fusion and potential anti-influenza drugs. Crystals of H14 HA soaked in a 5 μM solution of TBHQ for 30 min diffracted to a Bragg spacing of >2.5 Å. From *in silico* docking analyses TBHQ was suggested to bind to HA in a cavity near the fusion peptide (Fig. 5); however, electron density maps (Fig. 5A and B) clearly showed the compound bound uniquely, adjacent to the C terminus of the short α-helix of the HA2 α-helical hairpin (Fig. 5A). TBHQ was manually positioned into the electron density and then subjected to standard crystallographic refinement. The thermal factors for the atoms of TBHQ refined to similar values to those of the surrounding protein atoms, indicating that high site occupancy had been achieved.

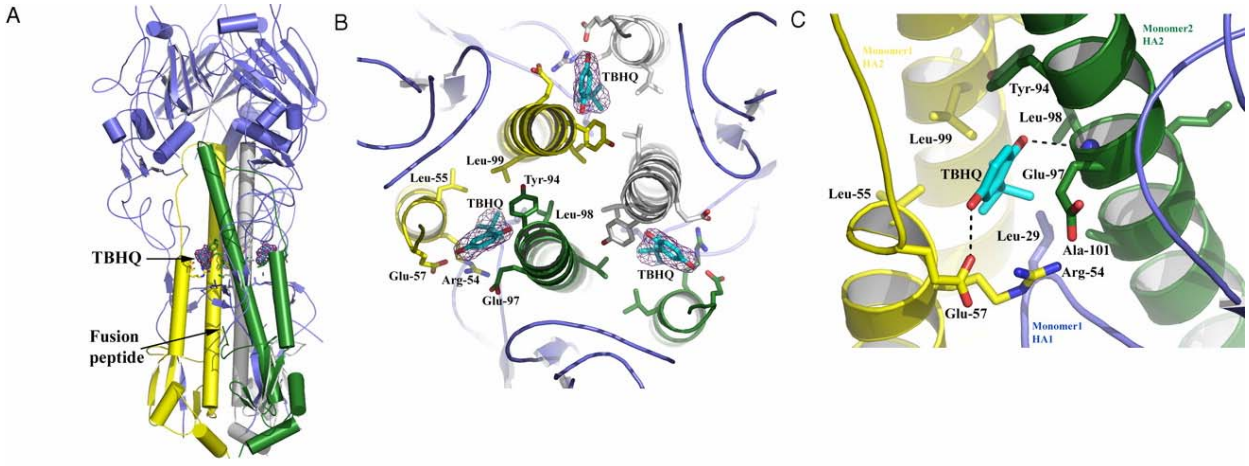

Fig. 5. The location and composition of the TBHQ binding site. (A) Representation of the H14 HA trimer. The 3 HA1s are colored in blue, and the 3 HA2s are in yellow, green, and gray. The locations of the 3 TBHQ molecules and the fusion peptide are highlighted. (B) View down the 3-fold axis of H14 HA to show the 3 TBHQ binding sites. A 2 Fo − Fc electron density map (contoured at 1σ) is shown for TBHQ. Selected residues are shown as sticks. The same color scheme as in A is used. (C) Close-up view of a single TBHQ binding site. Selected residues are shown as sticks, and potential hydrogen bonds are shown as dotted lines.

The TBHQ binding site is located at the interface between 2 monomers of the HA trimer, and there are therefore 3 TBHQ sites per trimer (Fig. 5B). The site is formed by residues from the long HA2 α-helices of each monomer (monomer 1 is colored in yellow and monomer 2 in green in Fig. 5) and from the short HA2 α-helix of monomer 2. Monomer 1 also fills in the bottom of the site via residue 291 of the

highly conserved β-hairpin of HA1 (residues 26–34). The interactions between TBHQ and HA are predominantly (85%) hydrophobic, largely accounted for by the highly hydrophobic base of the site, comprising the group-conserved residues Leu-291, Leu-982, and Ala-1012 of monomer 1, and Leu-552 and Leu-992 of monomer 2, into which the tert-butyl group of TBHQ packs (subscript 1 denotes a residue from HA1 and subscript 2 denotes a residue from HA2). There are 3 ionizable amino acids associated with the site: Arg-542 and Glu-572 from monomer 2 and Glu-972 from monomer 1. The conformations of Arg-542 and Glu-972 are such that the aliphatic parts of their side chains face the binding site, whereas the ionizable groups are oriented away from it. Indeed, the aliphatic side chain of Glu-972 packs across the face of the quinone ring of TBHQ. In contrast, the carboxyl group of Glu-572 is involved in a hydrogen-bond network with both the side chain and the main-chain carbonyl of Arg-542, and with the O1 oxygen of TBHQ. The other oxygen atom of TBHQ, O2, makes a hydrogen bond with the main-chain amide of Leu-982 (Fig. 5C). Presumably, these hydrogen bonds through which the short and long α-helices of the site are bridged, together with the hydrophobic interactions, enhance the stability of the HA trimer. Only O1 and the top of the quinone ring of bound TBHQ are partially accessible to solvent, because 90% of the surface area of TBHQ is solvent inaccessible. The binding site has a normalized complementarity of 0.7 (a value of 1 representing a perfect fit) [35].

As shown in Fig. 6, the 5 phylogenetic clades of HA fall into 2 groups. Previous studies have shown that membrane fusion by H3, but not H1, HAs is inhibited by TBHQ, suggesting that TBHQ may be a group 2-specific inhibitor [36]. Comparison of the crystal structures of group 1 and group 2 HAs in the vicinity of the TBHQ binding site reveals important structural differences that could account for the group-specific activity of the compound (Fig. 6). In group 1 HAs access, to what would be the TBHQ binding site, is blocked because of an extra turn at the C terminus of the short α-helix (residues 56–58). This additional turn of helix in group 1 HAs results from the formation of an intermonomer salt bridge between Lys-582 and Glu-972. In group 2 HAs this interaction is not made (although Lys-582 is conserved in all HAs) because Glu-972 prefers to form a salt bridge with the group 2-conserved residue Arg-542. Consequently, Lys-582 is not well ordered in group 2 HAs, and the TBHQ site is accessible.

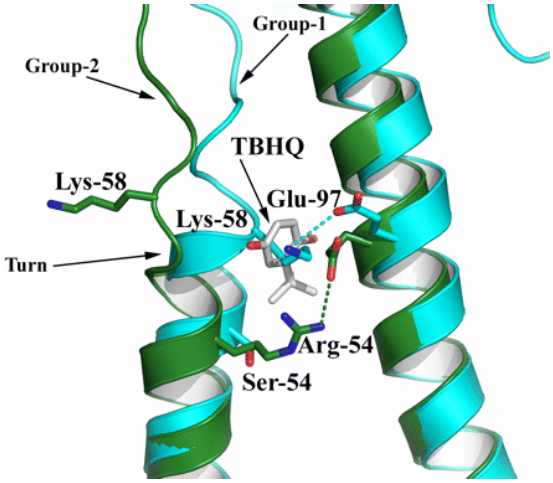

Fig. 6. The structural basis for HA group-specific inhibition by TBHQ. Superposition of H14 (green) and H5 (cyan) HAs clearly shows that the additional turn of helix A in the group 1 HAs precludes TBHQ binding. Potential hydrogen bonds are shown as dotted lines.

Based on the structure and activity of the template compound (TBHQ), Hoffman et al [37] have designed a series of novel HA2 inhibitors. The design involved (i) the recently refined crystal structure (2.1-Å resolution) of the HA ectodomain, (ii) new insights into the conformational change, and (iii) improvements in the molecular docking program, DOCK. As a result, authors identified new inhibitors of HA-mediated membrane fusion. Like TBHQ, most of these molecules inhibit the conformational change. One of the new compounds, however, facilitates rather than inhibits the HA conformational change. Nonetheless, the facilitator, diiodofluorescein, inhibits HA-mediated membrane fusion and, irreversibly, infectivity. The effects of inhibitors from both searches on the conformational change and membrane fusion activity of HA as well as on viral infectivity were also characterized. In addition, several mutants resistant to each class of inhibitor were isolated and described.

The region of HA (Fig. 7A) chosen for the new structure-based inhibitor search contains the interfaces between the globular heads (an inter-monomer interface) and those between HA1 and HA2 (intramonomer interface). Two neighboring sites were defined, referred to as 2A and 2B, and were used for independent searches. Site 1A, the pocket used in the original search that identified TBHQ, is also shown. Note that there are three copies of each site per trimer. The limits of the pockets of both sites 2A and 2B are partially defined by residues from HA2 54–81, the region of HA that undergoes a random coil-to-coiled-coil transition at low pH. Both sites exhibit many intermonomer and intramonomer interactions, involving both hydrophobic and polar contacts. Any of these interactions are potential targets for stabilization or destabilization by a small molecule. The sites were also chosen for their sizes, their concave shapes, and their high level of sequence conservation. For both sites, surface residues are 98% identical among all influenza viruses of the H3 subtype and 78% identical among all influenza A viruses.

Then, authors have tested 12 of the new compounds selected by DOCK (Fig. 7B) for their effects on the low-pH conformational change conformational change. Two other molecules that facilitate the conformational change were also identified. One (C29), however, was too toxic to determine its effect on infectivity, while the other (S23) had no measurable effect on infectivity (Table 3). Compound C22 was found to be the most potent from this series. C22 inhibited viral infectivity in the single-cycle growth assay with an IC_{50} of 8 μM, and it is not toxic to MDCK2 cells at this or higher concentrations. It was also found that both TBHQ and C22 inhibited RBC-cell fusion at 10 and 100 μM, the same range in which they inhibited conformational change and viral infectivity. The effects of TBHQ and C22 on the pH dependence of membrane fusion were investigated using a hemolysis assay.

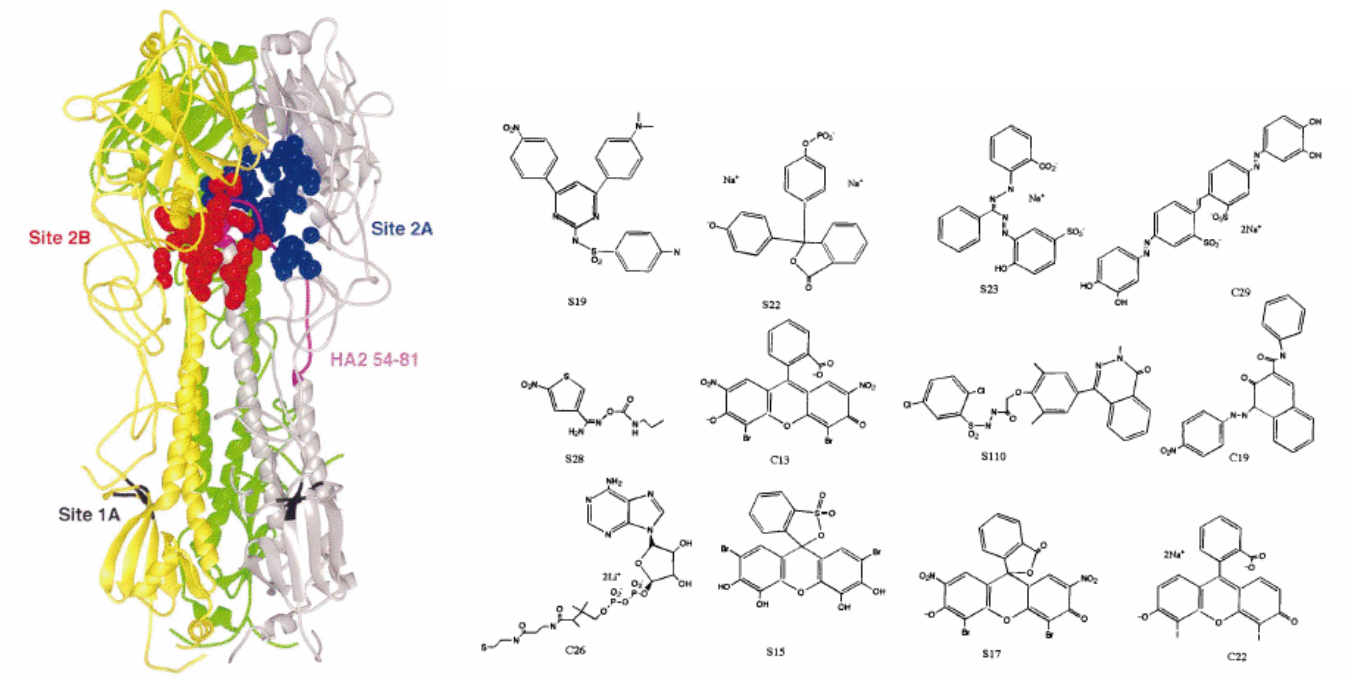

(**A**) (**B**)

Fig. 7. (**A**) Locations of new DOCK sites in the neutral-pH structure of BHA, a soluble trimeric HA ectodomain. The coordinates used are from the Brookhaven protein data bank, entry 5HMG. Monomers in the BHA trimer are colored gray, yellow, and green. Dots indicate locations of spheres used in orienting potential ligands computationally for evaluation of predicted interaction with a site. Blue dots, site 2A; red dots, site 2B; magenta, HA2 54-81: black area, site 1A; (**B**) Structures of compounds selected by DOCK as potential HA inhibitors. The C or S prefix indicates whether the compound came from DOCK output to site 2A or 2B, respectively.

Table 3. Effects of compounds targeted to new DOCK sites

Compound	IC_{50} (μM)[a]			Force field score[b]
	Conformational change	Infectivity	Cell viability	
TBHQ[c]	Inhibitor (12)	20.0	>100	−15.4
S19	Inhibitor (<100)	0.8	>>500	−38.1
S22	Inhibitor (<100)	40.0	>>100	−43.3
C22	Effector (8)	8.0	1,000	−41.9
S23	Effector (<100)	>100	100	−35.6
C29	Effector (<100)	ND[d]	<1	−43.0
S28	Inhibitor (<100)	>50	>50	−35.7
C13	Inhibitor (<100)	>100	>100	−41.1
C26	No effect	ND	ND	−39.8
S15	No effect	ND	ND	−35.1
S110	No effect	ND	ND	−36.7
C19	No effect	ND	ND	−40.9
S17	No effect	ND	ND	−34.6

[a]Effects on conformational change, infectivity, and cell viability were measured with the thermolysin, ELISA, and MTT assays, respectively; [b]Calculation of the DOCK force field score is as per the DOCK3.5 user's manual; a more negative value indicates a higher predicted affinity; [c]Values for the effects of TBHQ on conformational change (SPA assay), infectivity, and cell viability are from reference [38]; [d]ND, not determined.

Based on the data described above, for the design of our HA2-targeted library we have used a multi-step approach with the main focus on 3D-molecular docking.

Concept and Applications

HA2-targeted library design at CDL involves:

• *A combined profiling methodology that provides a consensus score and decision based on various advanced computational tools*:

1. Bioisosteric morphing, structure diversity & similarity concept, topological pharmacophore and funneling procedures in designing novel potential HA2 ligands with high IP value. We apply CDL's proprietary Chemosoft^{TM} software and commercially available solutions from Accelrys, MOE, Daylight and other platforms.

2. Neural Network tools for target-library profiling, in particular Self-organizing Kohonen Maps, performed in SmartMining Software.

3. 3D-molecular docking approach to focused library design.

4. Computational-based `*in silico*` ADME/Tox assessment for novel compounds includes prediction of human CYP P450-mediated metabolism and toxicity as well as many pharmacokinetic parameters, such as Brain-Blood Barrier (BBB) permeability, Human Intestinal Absorption (HIA), Plasma Protein binding (PPB), Plasma half-life time ($T_{1/2}$), Volume of distribution in human plasma (V_d), etc.

The fundamentals for these applications are described in a series of our recent articles on the design of exploratory small molecule chemistry for bioscreening [for related data visit ChemDiv. Inc. online source: www.chemdiv.com].

• *Synthesis, biological evaluation and SAR study for the selected structures*:

1. High-throughput synthesis with multiple parallel library validation. Synthetic protocols, building blocks and chemical strategies are available.

2. Library activity validation via bioscreening; SAR is implemented in the next library generation.

We practice a multi-step approach for building HA2-focused library:

Virtual screening

(1) The small-molecular ligands reported for HA2 are compiled into a unique knowledge base (*reference ligand space*). Based on the non-trivial bioisosteric approach, topological pharmacophores and targeted diversity concept more than 15K compounds have been added to the first rough library. Then, these compounds have been scored using 3D-molecular docking approach to create the final library.

3D-molecular Docking

Currently, several crystallographic complexes of HA2 with various peptides and several small-molecule compounds are available in PDB databank. This data and molecular docking studies described above have been used for the active site construction, 3D-modeling and virtual scoring generation. The constructed HA-binding active sites are shown in Fig. 8.

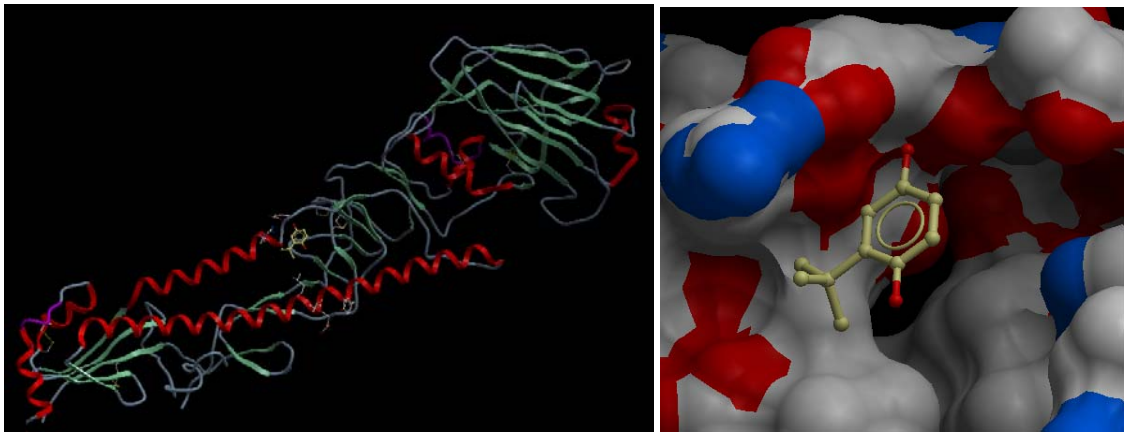

Fig. 8. Crystallographic data for the single subunit of HA with TBHQ in the active binding HA2/HA1-site.

We have scored the ChemDiv structures outputted from the previous step using the developed models. As a result more than 5K compounds successfully passed through the HA model and have grouped into the four different categories: *inactive*, *low, medium*, *high*. Compounds from the last three categories were included in the final library (Fig. 9). Representative examples of small-molecule ChemDiv compounds included in the final HA2-targeted library are shown in Fig. 10.

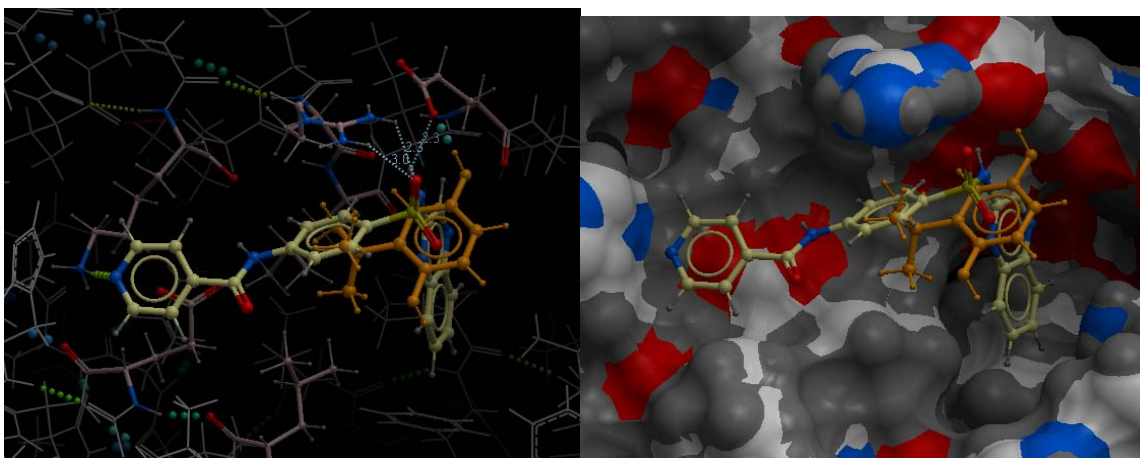

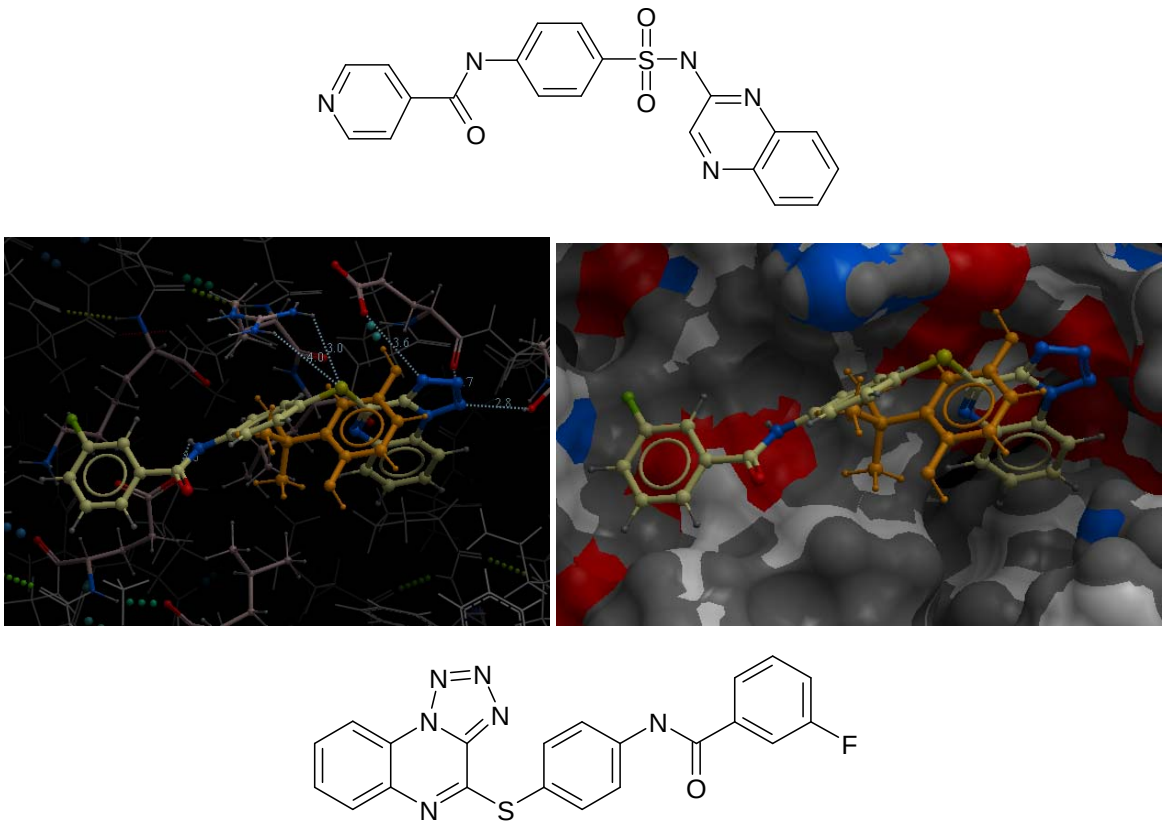

Fig. 9. Representative examples of compounds successfully passed the docking procedure.

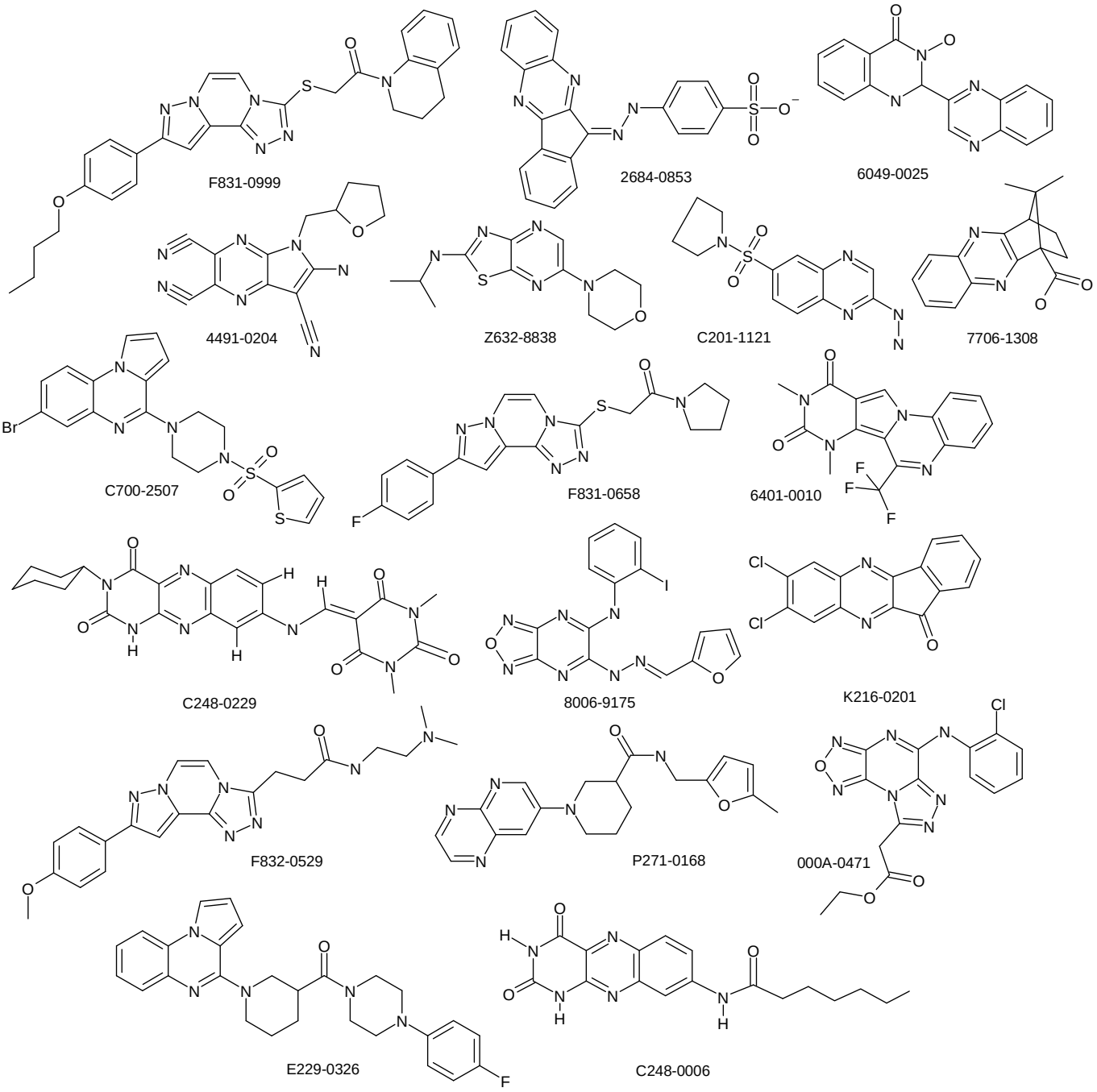

Fig. 10. Representative examples of structures from HA2-targeted library.

As a result of the performed CADD, we have selected approx. 5K small-molecule compounds which are the main content of the final HA2-focused library. We also provide rapid and efficient tools for follow-up chemistry on discovered hits. Targeted library is updated quarterly based on a "cache" principle. Older scaffolds/compounds are replaced by templates resulting from our *in-house* development (unique chemistry, literature data, CADD) while the overall size of the library remains the same (ca. 5-8K compounds). As a result, the library is renewed each year, proprietary compounds comprising 50-75% of

the entire set. Clients are invited to participate in the template selection process prior to launch of our synthetic effort.

References

[1] Fan J, et al. Preclinical study of influenza virus A M2 peptide conjugate vaccines in mice, ferrets, and rhesus monkeys. Vaccine. 2004;22:2993–3003

[2] Horimoto T, Kawaoka Y. Influenza: Lessons from past pandemics, warnings from current incidents. Nat Rev Microbiol. 2005;3:591–600.

[3] Wiley DC, Wilson IA, Skehel JJ. Structural identification of the antibody-binding sites of Hong Kong influenza haemagglutinin and their involvement in antigenic variation. Nature. 1981;289:373–378

[4] Gocnik M, et al. Antibodies induced by the HA2 glycopolypeptide of influenza virus haemagglutinin improve recovery from influenza A virus infection. J Gen Virol. 2008;89:958–967 Smirnov YA, Lipatov AS, Gitelman AK, Class EC, Osterhaus AD. Prevention and treatment of bronchopneumonia in mice caused by mouse-adapted variant of avian H5N2 influenza A virus using monoclonal antibody against conserved epitope in the HA stem region. Arch Virol. 2000;145:1733–1741 Okuno Y, Matsumoto K, Isegawa Y, Ueda S. Protection against the mouse-adapted A/FM/1/47 strain of influenza A virus in mice by a monoclonal antibody with cross-neutralizing activity among H1 and H2 strains. J Virol. 1994;68:517–520

[5] Ekiert DC, et al. Antibody recognition of a highly conserved influenza virus epitope. Science. 2009;324:246–251 Sui J, et al. Structural and functional bases for broad-spectrum neutralization of avian and human influenza A viruses. Nat Struct Mol Biol. 2009;16:265–273. Throsby M, et al. Heterosubtypic neutralizing monoclonal antibodies cross-protective against H5N1 and H1N1 recovered from human IgM+ memory B cells. PLoS One. 2008;3:e3942 Okuno Y, Isegawa Y, Sasao F, Ueda S. A common neutralizing epitope conserved between the hemagglutinins of influenza A virus H1 and H2 strains. J Virol. 1993;67:2552–2558 Sanchez-Fauquier A, Villanueva N, Melero JA. Isolation of cross-reactive, subtype-specific monoclonal antibodies against influenza virus HA1 and HA2 hemagglutinin subunits. Arch Virol. 1987;97:251–265

[6] Hernandez, L.D., Hoffman, L.R., Wolfsberg, T.G. & White, J.M. Annu. Rev. Cell Dev. Biol. 12, 627−661 (1996)

[7] Durrer, P. et al. J. Biol. Chem. 271, 13417−13421 (1996)

[8] Durell, S.R., Martin, I., Ruysschaert, J.M., Shai, Y. & Blumenthal, R. Mol. Membr. Biol. 14, 97−112 (1997)

[9] Skehel JJ, Wiley DC. Receptor binding and membrane fusion in virus entry: The influenza hemagglutinin. Annu Rev Biochem. 2000;69:531–569

[10] Wilson, I.A., Skehel, J.J. & Wiley, D.C. Nature 289, 366−373 (1981)

[11] Chen, J., Skehel, J.J. & Wiley, D.C. Proc. Natl. Acad. Sci. USA 96, 8967−8972 (1999)

[12] Bullough, P.A., Hughson, F.M., Skehel, J.J. & Wiley, D.C. Nature 371, 37−43 (1994)

[13] Bullough, P.A., Hughson, F.M., Skehel, J.J. & Wiley, D.C. Nature 371, 37−43 (1994)

[14] Carr, C.M. & Kim, P.S. Cell 73, 823−832 (1993)

[15] Chen, J., Skehel, J.J. & Wiley, D.C. Proc. Natl. Acad. Sci. USA 96, 8967−8972 (1999)

[16] Chen, J., Skehel, J.J. & Wiley, D.C. Proc. Natl. Acad. Sci. USA 96, 8967−8972 (1999)

[17] Melikyan, G.B. et al. J. Cell Biol. 151, 413−424 (2000)

[18] Jin, H., Leser, G.P. & Lamb, R.A. EMBO J. 13, 5504−5515 (1994)

[19] Kuzmin, P.I., Zimmerberg, J., Chizmadzhev, Y.A. & Cohen, F.S. Proc. Natl. Acad. Sci. USA 98, 7235−7240 (2001)

[20] Chen J, et al. Structure of the hemagglutinin precursor cleavage site, a determinant of influenza pathogenicity and the origin of the labile conformation. Cell. 1998;95:409–417. Bullough PA, Hughson FM, Skehel JJ, Wiley DC. Structure of influenza haemagglutinin at the pH of membrane fusion. Nature. 1994;371:37–43. Sauter NK, et al. Binding of influenza virus hemagglutinin to analogs of its cell-surface receptor, sialic acid: Analysis by proton nuclear magnetic resonance spectroscopy and X-ray crystallography. Biochemistry. 1992;31:9609–9621. Wilson IA, Skehel JJ, Wiley DC. Structure of the haemagglutinin membrane glycoprotein of influenza virus at 3 A resolution. Nature. 1981;289:366–73.

[21] Kim CS, Epand RF, Leikina E, Epand RM, Chernomordik LV. The final conformation of the complete ectodomain of the HA2 subunit of influenza hemagglutinin can by itself drive low pH-dependent fusion. J Biol Chem. 2011 Apr 15;286(15):13226-34

[22] Bommakanti G, Citron MP, Hepler RW, Callahan C, Heidecker GJ, Najar TA, Lu X, Joyce JG, Shiver JW, Casimiro DR, ter Meulen J, Liang X, Varadarajan R. Design of an HA2-based Escherichia coli expressed influenza immunogen that protects mice from pathogenic challenge. Proc Natl Acad Sci U S A. 2010 Aug 3;107(31):13701-6

[23] De Clercq, E. 2006. Antiviral agents active against influenza A viruses. Nat. Rev. Drug Discov. 5:1015-1025

[24] Bright, R. A., M. J. Medina, X. Xu, G. Perez-Oronoz, T. R. Wallis, X. M. Davis, L. Povinelli, N. J. Cox, and A. I. Klimov. 2005. Incidence of adamantane resistance among influenza A (H3N2) viruses isolated worldwide from 1994 to 2005: a cause for concern. Lancet 366:1175-1181 Deyde, V. M., X. Xu, R. A. Bright, M. Shaw, C. B. Smith, Y. Zhang, Y. Shu, L. V. Gubareva, N. J. Cox, and A. I. Klimov. 2007. Surveillance of resistance to adamantanes among influenza A(H3N2) and A(H1N1) viruses isolated worldwide. J. Infect. Dis. 196:249-257

[25] Moscona, A. 2008. Medical management of influenza infection. Annu. Rev. Med. 59:397-413.

[26] de Jong, M. D., T. T. Tran, H. K. Truong, M. H. Vo, G. J. Smith, V. C. Nguyen, V. C. Bach, T. Q. Phan, Q. H. Do, Y. Guan, J. S. Peiris, T. H. Tran, and J. Farrar. 2005. Oseltamivir resistance during treatment of influenza A (H5N1) infection. N. Engl. J. Med. 353:2667-2672 Kiso, M., K. Mitamura, Y. Sakai-Tagawa, K. Shiraishi, C. Kawakami, K. Kimura, F. G. Hayden, N. Sugaya, and Y. Kawaoka. 2004. Resistant influenza A viruses in children treated with oseltamivir: descriptive study. Lancet 364:759-765

[27] Schunemann, H. J., S. R. Hill, M. Kakad, R. Bellamy, T. M. Uyeki, F. G. Hayden, Y. Yazdanpanah, J. Beigel, T. Chotpitayasunondh, C. Del Mar, J. Farrar, T. H. Tran, B. Ozbay, N. Sugaya, K. Fukuda, N. Shindo, L. Stockman, G. E. Vist, A. Croisier, A. Nagjdaliyev, C. Roth, G. Thomson, H. Zucker, and A. D. Oxman. 2007. WHO rapid advice guidelines for pharmacological management of sporadic human infection with avian influenza A (H5N1) virus. Lancet Infect. Dis. 7:21-31 Shinde, V., C. B. Bridges, T. M. Uyeki, B. Shu, A. Balish, X. Xu, S. Lindstrom, L. V. Gubareva, V. Deyde, R. J. Garten, M. Harris, S. Gerber, S. Vagasky, F. Smith, N. Pascoe, K. Martin, D. Dufficy, K. Ritger, C. Conover, P. Quinlisk, A. Klimov, J. S. Bresee, and L. Finelli. 2009. Triple-reassortant swine influenza A (H1) in humans in the United States, 2005-2009. N. Engl. J. Med. 360:2616-2625

[28] Skehel, J. J., and D. C. Wiley. 2002. Influenza haemagglutinin. Vaccine. 20(Suppl. 2):S51-S54.

[29] Hoffman LR, Kuntz ID, White JM (1997) Structure-based identification of an inducer of the low-pH conformational change in the influenza virus hemagglutinin: Irreversible inhibition of infectivity. J Virol 71:8808–8820 Bodian DL, et al. (1993) Inhibition of the fusion-inducing conformational change of influenza hemagglutinin by benzoquinones and hydroquinones. Biochemistry 32:2967–2978. Yu KL, et al. (2002) Structure-activity relationships for a series of thiobenzamide influenza fusion inhibitors derived from 1,3,3-trimethyl-5-hydroxy-cyclohexylmethylamine. Bioorg Med Chem Lett 12:3379–3382.

[30] Vanderlinden E, Göktas F, Cesur Z, Froeyen M, Reed ML, Russell CJ, Cesur N, Naesens L Novel inhibitors of influenza virus fusion: structure-activity relationship and interaction with the viral hemagglutinin. J Virol. 2010 May;84(9):4277-88.

[31] Luo, G., R. Colonno, and M. Krystal. 1996. Characterization of a hemagglutinin-specific inhibitor of influenza A virus. Virology 226:66-76 Plotch, S. J., B. O'Hara, J. Morin, O. Palant, J. LaRocque, J. D. Bloom, S. A. Lang, Jr., M. J. DiGrandi, M. Bradley, R. Nilakantan, and Y. Gluzman. 1999. Inhibition of influenza A virus replication by compounds interfering with the fusogenic function of the viral hemagglutinin. J. Virol. 73:140-151

[32] Richards, F. M. 1977. Areas, volumes, packing and protein structure. Annu. Rev. Biophys. Bioeng. 6:151-176

[33] Liu S, Li R, Zhang R, Chan CC, Xi B, Zhu Z, Yang J, Poon VK, Zhou J, Chen M, Münch J, Kirchhoff F, Pleschka S, Haarmann T, Dietrich U, Pan C, Du L, Jiang S, Zheng B. CL-385319 inhibits H5N1 avian influenza A virus infection by blocking viral entry. Eur J Pharmacol. 2011 Jun 25;660(2-3):460-7

[34] Rupert J. Russella, Philip S. Kerrya, David J. Stevens, David A. Steinhauer, Stephen R. Martin, Steven J. Gamblin, and John J. Skehel. Structure of influenza hemagglutinin in complex with an inhibitor of membrane fusion Proc Natl Acad Sci U S A. 2008 Nov 18;105(46):17736-41

[35] Sobolev V, Sorokine A, Prilusky J, Abola EE, Edelman M (1999) Automated analysis of interatomic contacts in proteins. Bioinformatics 15:327–332

[36] Shangguan T, Alford D, Bentz J (1996) Influenza virus-liposome lipid mixing is leaky and largely insensitive to the material properties of the target membrane. Biochemistry 35:4956–4965

[37] Hoffman LR, Kuntz ID, White JM. Structure-based identification of an inducer of the low-pH conformational change in the influenza virus hemagglutinin: irreversible inhibition of infectivity. J Virol. 1997 Nov;71(11):8808-20.

[38] Bodian, D. L., R. B. Yamasaki, R. L. Buswell, J. F. Stearns, J. M. White, and I. D. Kuntz. 1993. Inhibition of the fusion-inducing conformational change of influenza hemagglutinin by benzoquinones and hydroquinones. Biochemistry 32:2967–2978.